The properties and removal efficacies of natural organic matter fractions by South African drinking water treatment plants

Moyo, Welldone; Chaukura, Nhamo; Msagati, Titus A.M.; Mamba, Bhekie B.; Heijman, Sebastian G.J.; Nkambule, Thabo T.I.

DOI
10.1016/j.jece.2019.103101

Publication date
2019

Document Version
Final published version

Published in
Journal of Environmental Chemical Engineering

Journal of Environmental Chemical Engineering 7 (2019) 103101

Contents lists available at ScienceDirect

Journal of Environmental Chemical Engineering

journal homepage: www.elsevier.com/locate/jece

The properties and removal efficacies of natural organic matter fractions by South African drinking water treatment plants

Welldone Moyo[a], Nhamo Chaukura[a], Titus A.M Msagati[a], Bhekie B. Mamba[a], Sebastian G.J Heijman[b], Thabo T.I Nkambule[a,*]

[a] Nanotechnology and Water Sustainability (NanoWS) Research Unit, University of South Africa, Johannesburg, South Africa
[b] Department of Civil Engineering and GeoSciences, Technical University of Delft, Delft, the Netherlands

ARTICLE INFO

Keywords:
Drinking water treatment
Fluorescence excitation-emission matrices
Fluorescent natural organic matter
Parafac
Polysaccharides

ABSTRACT

This study presents an investigation on the fate of natural organic matter (NOM) and its dynamics throughout the treatment train at various drinking water treatment plants (WTP) in South Africa. The characteristics, concentration and removal efficiencies of NOM at various treatment stages on the basis of dissolved organic carbon, UV absorbance, specific ultra-violet absorbance, spectroscopic indices, maximum fluorescence intensity (*Fmax*), and polysaccharides removal, were studied. The highest polysaccharide concentration was in coastal plants compared to inland plants for the raw water samples. A Parafac model fitting four components was established for the raw waters, and validated based on the split half criteria. The *Fmax* values of the components was higher for terrestrial humic-like component (C1) and fulvic-like component (C2) than for humic-like components (C3), and for protein-like component (C4). Strikingly, the mean *Fmax* values for C2 and C3 were higher for plants located on the south west coast of South Africa than the plants located inland. While the humification index and UV_{254} removal correlated (R^2 = 0.797), the correlation between the freshness index (β:α) and UV_{254} removal was also mild (R^2 = 0.787). The removal efficiencies of bulk NOM were higher than for FNOM in the rapid sand filtration (RSF) stage, regardless of the location of the plants, suggesting that the RSF process is more efficient in removing non-fluorescent NOM than FNOM fractions. This study demonstrated the capability of optical methods in characterizing the fate, occurrence and removal of NOM in surface waters.

1. Introduction

Recently, natural organic matter (NOM) has attracted significant research attention because it compromises the performance of water treatment plants (WTPs). Natural organic matter affects the efficiency of water treatment stages such as the coagulation-flocculation [1], and potentially leads to the generation of disinfection by-products (DBPs) [2–4]. Optimization of treatment processes for the removal of NOM requires data on its characteristics and seasonal variation in the water source [5]. Conventional WTPs, which are commonly used in developing countries such as South Africa, are not designed to remove NOM [6,7]. Moreover, the removal of NOM is costly, hence the need to track temporal changes of its quality using online monitoring techniques. Many WTPs in South Africa depend solely on specific UV absorbance (SUVA) to assess the quality of NOM [8]. However, a similar SUVA value does not always translate to similar reactivity; these values may differ in their distribution around an average value. Therefore comprehensive and sensitive analytical approaches are required to provide more detail on the reactivity and treatability of NOM.

On the one hand, fluorescence spectroscopy is a rapid and user-friendly technique that provides detailed analytical information. This technique can discriminate between diverse types of NOM based on light scattering properties upon irradiation of the fluorophores [9]. Combining fluorescence data with routine water quality monitoring data such as dissolved organic carbon (DOC) and ultraviolet absorbance (UVA) can be effective in determining the origin of NOM and evaluating a treatment process [10]. When applied in the three-dimensional mode, fluorescence produces an emission excitation matrix (EEM), which provides a spectral signature of the fluorescent NOM [11]. EMMs contain large volumes of intricate data, whose explanation can be difficult [12–15]. Identification of fluorescence peaks and comparison of the intensities of individual peaks by visual inspection of the fluorescence maps is a commonly used technique. Recently, chemometric techniques such as parallel factor analysis (Parafac) and fluorescence regional integration (FRI) have been used to elucidate the wavelength-dependent fluorescence intensity data points embedded in EEMs [16].

* Corresponding author.
E-mail address: nkambtt@unisa.ac.za (T.T.I. Nkambule).

https://doi.org/10.1016/j.jece.2019.103101
Received 14 January 2019; Received in revised form 28 March 2019; Accepted 17 April 2019
Available online 18 April 2019
2213-3437/

On the other hand, the source, composition, and reactivity of chromophoric DOC (CDOM) has been traced in natural waters using UV–vis spectroscopy [17]. Furthermore, differences in the feed water and impact of treatment at each stage in the treatment train on the water quality, have been followed using indices derived from UVA, DOC, SUVA, and fluorescence [18]. Opportunities for rapid and practical use of these indices can be enhanced by automating and performing online analyses, which increase the safety, responsiveness, and treatment precision on plant operations. Moreover, the analysis of biogenic NOM in water research uses the high performance liquid chromatography with on-line organic carbon detection (LC-OCD) technique, which is costly and laborious. In view of this, the present work uses the sulfuric acid–UV method, which is a rapid and accurate method for determining the fluorescent fractions of NOM.

To date, only a few studies on the character of NOM found in water treatment plants in South Africa have characterized NOM occurring at individual plants (e.g., [19,20,6]. This work is the first in South Africa to report on the occurrence, behavior and removal efficiencies of fluorescent EEM components throughout the water treatment processes. It is of interest therefore, to assess the treatment efficiency of these plants for the treatment of NOM, given the variability of the water types in South Africa [21]. It is expected that the water types influence the occurrence of NOM components, and the treatment regimen at the plants in turn influences the behavior and removal efficiency of NOM components.

Nine WTPs in different regions were sampled with the objectives of: (1) characterizing NOM parameters and identifying the correlation between NOM composition and optimal NOM removal at the respective sites, (2) examining the input of individual NOM components to the overall fluorescent NOM in treated water of dynamic quality throughout the treatment train, and (3) determining the process robustness and/or selectivity in the removal of fluorescent NOM components.

2. Materials and methods

The study was composed of two distinct phases. Phase I was an assessment of the spatial changes on NOM in raw water at abstraction points of all plants, while phase II evaluated variations of NOM concentrations after treatment at various unit processes for each WTP.

2.1. Sampling

Sampling was conducted at nine water treatment plants representative of the five water quality regions found in South Africa (Fig. 1) using clean 1L glass bottles with Teflon lined caps. Triplicate samples were obtained after each major treatment step, namely: raw, flocculation/coagulation, settling, rapid sand filtration, and disinfection (Fig. A1). Turbidity, pH, temperature, and conductivity were measured onsite using potable multimeters. The samples were transported in ice boxes and then immediately filtered using a 0.45 µm GF/F filters before storage at 4 °C and analysed within 48 h. Filtered samples were analysed for DOC using a total organic carbon analyser (Teledyne Tekmar, TOC fusion).

2.2. Fluorescence and UV absorbance analysis

Triplicate water samples taken after each treatment stage were filtered through a 0.45 µm filter and equilibrated to 25 °C before analysis. Fluorescence EEMs, absorbance spectra, and simulated synchronous scans at $\Delta\lambda = 60$ nm, were obtained using a fluorescence spectrometer (Aqualog, HORIBA, Jobin Yvon) in the wavelength range 200–800 nm at 2 nm excitation intervals, and 248.58–830.59 nm at 3.28 nm emission intervals.

Parameters such as SUVA were derived by DOC normalization of UV_{254} absorbance and dimensionless indices such as the fluorescence index *(FI)*, humification index *(HIX)*, and freshness index *(β:α)* were calculated (Box 1). Higher *HIX* values are indicative of a greater extent of humification of the NOM. The *FI* index indicates the origin of the NOM, where a smaller value (< 1.3) indicates microbial source, while a greater value (around 1.8) means the NOM is of terrestrial origin. The *β:α* index indicates the age or extent of decomposition, and a high value indicates freshly produced NOM [22].

2.3. Fluorescence regional integration of removed fractions

The fluorescence regional integration method was applied in the identification and quantification of individual fluorescent components from the EEM spectra. Precisely, the EEM spectra were divided into five wavelength-dependent regions representative of where the maximum fluorescence occurs for each chemical standard used. The standards used had the same character as specific components of NOM (aromatic protein I, aromatic proteins II, microbial by-products, humic-like, and fulvic-like). The volume under region *i*, was calculated using Eq. 1 [23]:

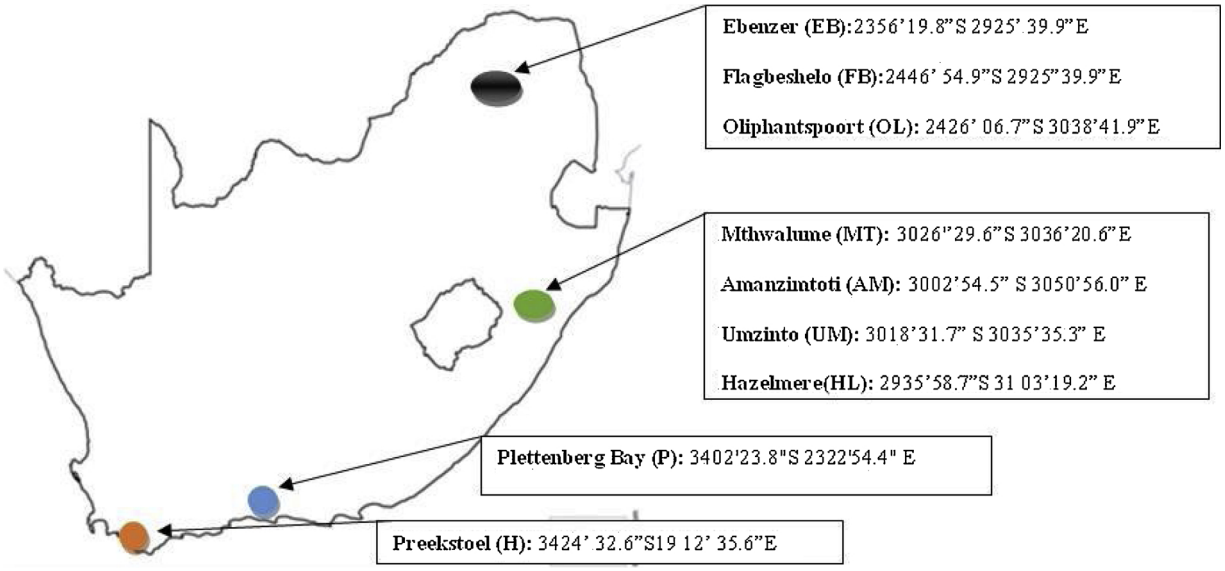

Fig. 1. The location of selected WTPs in South Africa.

Box 1
Spectroscopic indices for NOM characterization

$$SUVA\left(\frac{L}{mgM}\right) = \frac{UV_{254}(cm^{-1})}{DOC\left(\frac{mg}{L}\right)} x100$$

$$HIX = \sum I_{435\rightarrow480} / \left(\sum I_{300\rightarrow345} + \sum I_{435\rightarrow480}\right)$$

$$FI = Em_{470}/Em_{520}$$

$$\beta: \alpha = Em_{380}/\max(Em_{420\rightarrow}435)$$

$$\theta_i = \sum_{ex} \sum_{em} I(\lambda_{ex}\lambda_{ex})\Delta d\lambda_{ex} \Delta\, d\lambda_{em} \quad (1)$$

Where $\theta_i$is the volume under region I, $I(\lambda_{ex}\lambda_{em})$ is the fluorescence intensity at the excitation-emission wavelength ($\lambda_{ex}\lambda_{em}$)pairs, $\Delta d\lambda_{ex}$ and $\Delta d\lambda_{em}$ are the excitation, and emission wavelength increments, respectively.

The study used $\Delta\lambda = 2$ nm for both excitation and emission wavelengths increments. The quantity of the respective component is proportional to the volume under the curve. The percentage volume expressed for region *i* was calculated using Eqs. 2 and 3 [23]:

$$\theta_{Tot,5} = \sum_{i=1}^{5} \theta i_{i,5} \quad (2)$$

$$P_{i,n} = \frac{\theta_{i,5}}{\theta_{Tot,5}} * 100\% \quad (3)$$

Where, $\theta_{Tot,5}$ is the total volume of all the five regions. The specific region is denoted by number *n*; and $P_{i,n}$ is the percentage volume of specific region *i*.

FRI was applied in the quantification of fractions making up the differential EEMs (ΔEEM) (Eq. 4):

$$\Delta EEM = EEM \text{ of removed FDOM} = EEM_{before} - EEM_{after} \quad (4)$$

2.4. The sulphuric acid-UV absorbance method for polysaccharide quantification

The procedure for the proposed sulfuric acid–UV method was adopted from Albalasmeh et al. [24]. Briefly, 3 mL of concentrated sulphuric acid was added to a 1 mL aliquot of sample and cooled in ice to bring it to room temperature. Thereafter, the sample was vortexed for 30 s before UV analysis at 315 nm using a UV spectrophotometer (Lambda 650S, PerkinElmer).

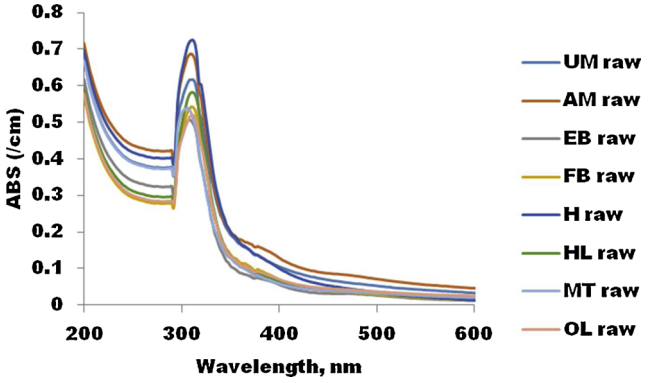

Fig. 2. UV absorbance after the sulfuric acid-UV method.

3. Results and discussion

3.1. Occurrence and distribution of fluorescence NOM components at source

3.1.1. Pseudo-quantitative determination of polysaccharides in raw water

UV-visible scans from 200 to 600 nm of samples prepared after the sulphuric acid-UV method [24] is presented in Fig. 2. The maximum absorbance peaks are slightly at shorter wavelength than that reported by Albalasmeh et al. [24]. In their work, they used pure carbohydrate samples whereas in this work real water samples were used, possibly containing a variety of carbohydrates. This slight hypsochromic shift arises because the range of chromophores that absorb in UV–vis region is high with varied concentrations giving rise to undistinguishable absorption spectra [25,26]. Additionally, molecular and intermolecular interactions, vibration and rotation distort the absorption spectral signatures in the UV spectrum [25,27]. However, for consistency with literature, UV absorbance at 315 nm was used for discussion, and the results are indicative rather than absolute.

Plant H exhibited the highest UV_{315} absorbance (0.73 cm^{-1}) and EB the lowest (0.46 cm^{-1}) (Fig. 2). Overall, the highest UV_{315} absorbance occurred in coastal compared to inland plants for the raw water samples. There was a strong correlation ($R^2 = 0.93$) between the UV_{315} and the *FI* spectroscopic ratios (Fig A. 2a), suggesting that the source of polysaccharides in the samples is of aquatic origin due to microbial activities releasing extracellular polymeric substances [28]. Costal plants have low *FI* index, indicating that microbial NOM has a high UV_{315} absorbance with high polysaccharide content. Polysaccharides are of interest to WTPs because they have a high membrane fouling propensity caused by their large molecular size and gelling properties, which enhance filtration resistance and attract bacteria to adhere to the membranes [29]. Thus costal plants intending to incorporate membrane technology must consider this implication critically.

3.1.2. 2D synchronous fluorescence spectra for raw water

Using 2D-SFS scans, one major peak and three broad shoulders were observed for all water sources (Fig. 3a). The protein like fluorescence (PLF) peak, which is associated with the presence of tyrosine-like and tryptophan-like components, was in the wavelength region 260–314 nm [30]. The microbial humic-like fluorescence (MHLF) component was the first shoulder in the wavelength range 314–355 nm [31], and the fulvic-like fluorescence (FLF) component was the second shoulder (355–420 nm) [32]. The humic-like fluorescence (HLF) component was the third and weak shoulder in the wavelength range 420–500 nm [33]. The 2D-SFS scan was able to resolve one peak and three shoulders, denoted as PLF, MHLF, FLF, and HLF, respectively. The area under each fluorescent region is proportional to the relative abundance of the fluorescent component in that region [31].

The variation of FLF and HLF follow a similar trend with the highest mean FLF area being that of a coastal plant, H (277.92 RU), which was about 5 times greater than the least, MT (76.03 RU).The raw water feeding plant H had high DOC (6.03 mg/L C) and high turbidity (5.32 NTU), indicating high quantities of colloidal and clay material [5].

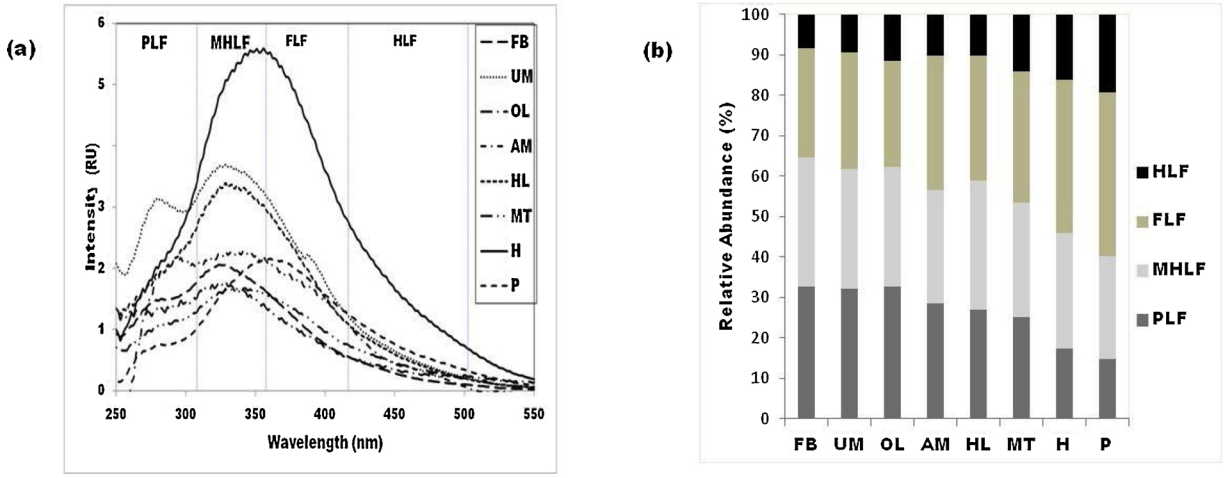

Fig. 3. (a) Synchronous scan of raw water sources, (b) relative abundance of NOM fractions in the raw water samples.

Water laden with humic acid and fulvic acid is characterized by a brownish-yellow coloration, typical of the surface water on the south-west coast of South Africa [5]. The mean MHLF and PLF areas for plant H (209.78 and 127.50 RU, respectively) were the highest and more than doubled the least plant, MT (66.05 and 58.89 RU, respectively). Although MT had the least MHLF area, it had the highest DOC value (12.51 mg/L C), further confirming the heterogeneity of the NOM. These results suggest raw water at MT (*FI* = 1.53) is of less microbial origin than at H (*FI* = 1.37), and that the source of DOC at MT is largely non fluorescent, containing mainly biopolymers, which are not easily assimilable by microorganisms [34,35]. Humic-like and fulvic-like material act as substrates for microbial growth, and thus support the survival of microorganisms [36,37]. Similar results were obtained on investigatiing biodegradable organic carbon (BDOC) for various WTPs in South Africa [5]. Plant H exhibited a high BDOC fraction (5 mg/L C) compared to other plants, which averaged 2 mg/L C.

3.1.3. Fluorescent dissolved organic matter components and their distribution at source

Parafac analysis was conducted using the Aqualog inbuilt SOLO software to study the quantitative removal of FDOM in detail. The Parafac model was built from the data acquired from all drinking water sources save for EB because its inclusion resulted in invalidated results when the split half analysis was used. For all water sources, modeling was carried out to maximize data collection and data points with the aim of deriving components which represented universal variance between water sources. The objective was to assess the occurrence and distribution of fluorescent components at source and draw correlations with other water quality parameters for predicting occurrence and treatability.

Fig. 4a shows the spectral signatures of the obtained components. The OpenFluor database was used to cross-reference the derived fluorescence components against those obtained globally [38]. This is however, a guideline, and the components identified in the study are not necessarily from similar origins. Similarity scores greater than 0.97 were found for each of the four identified components (Table 1).

A model fitting four components was established and validated based on the split half criteria as described by Murphy et al. [9], and Ndiweni et al. [39]. After validation, the distribution of the components at each water source was quantified using their maximum fluorescence intensities *(Fmax)*. The value of *Fmax* was higher for terrestrial humic-like component (C1) and fulvic-like component (C2) than for humic-like components (C3), and for protein-like (C4) components (Fig. 4e), suggesting C1 and C2 have high quantum efficiencies and low responses to quenching effects compared to C3 and C4 [40]. Strikingly, *Fmax* for C2 and C3 was higher for plants located on the south west coast of the country (P and H) than the other plants. The raw water feeding these plants has a brown-yellow coloration, characteristic of the presence of

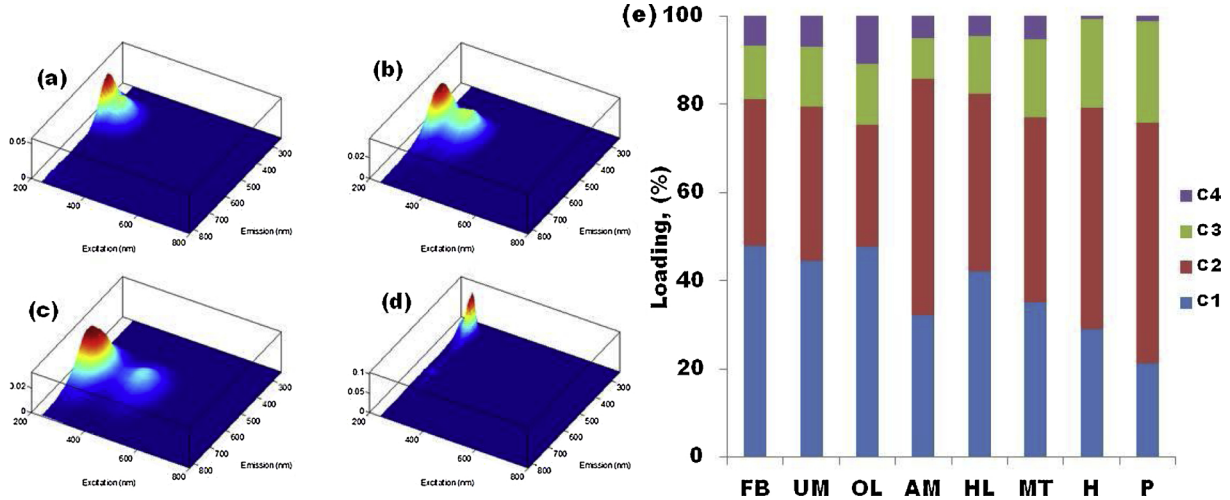

Fig. 4. Validated fluorescent components derived from the Parafac model on drinking water sources showing (a) component 1 (C1), (b) component 2 (C2), (c) component 3 (C3), and (d) component 4 (C4), and (e) the *Fmax* distribution of each component.

Table 1
Identities of similar components using the OpenFluor database.

Component	λ_{ex} (nm)	λ_{em} (nm)	Similarity score[a]	Component Identity	Reference
C1	316	< 240 (292)	0.97	Terrestrial humic like, reprocessed organic matter	[16]
			0.98	Humic-like, possible photo degradation product	
C2	336	< 240 (348)	0.98	Soil derived fulvic acid like	
C3	364	< 240 (450)	0.97	Humic acid like	
			0.98	Aromatic, conjugated macromolecular substances of terrestrial origin.	
C4	270	270	0.99	Protein, tryptophan-like	
			0.98	tryptophan-like	

Table 2
Dissolved organic carbon and spectrophotometric parameters for raw water sources *(n = 3)*.

Plant	C1	F_{max} (RU) C2	C3	C4	tCDOM (nm/cm)	a315 (/cm)	TotAbs /DOC (nm.mg/L.cm)	SUVA (L/mg.m)	UV254 (/cm)	DOC (mg/L)
FB	0.010	0.007	0.003	0.001	5.882	0.514	1.061	1.692	0.094	5.544
UM	0.009	0.007	0.003	0.001	9.360	0.578	1.242	1.872	0.141	7.535
OL	0.009	0.005	0.003	0.002	16.351	0.497	2.723	3.018	0.181	6.005
AM	0.005	0.008	0.001	0.001	16.224	0.638	3.436	3.896	0.184	4.721
HL	0.009	0.008	0.003	0.001	12.768	0.558	4.912	6.339	0.165	2.600
MT	0.007	0.008	0.003	0.001	12.012	0.463	0.960	1.117	0.140	12.509
H	0.006	0.010	0.004	0.000	35.935	0.674	5.960	7.988	0.482	6.030
P	0.004	0.010	0.004	0.000	19.572	0.643	3.328	4.379	0.258	5.881

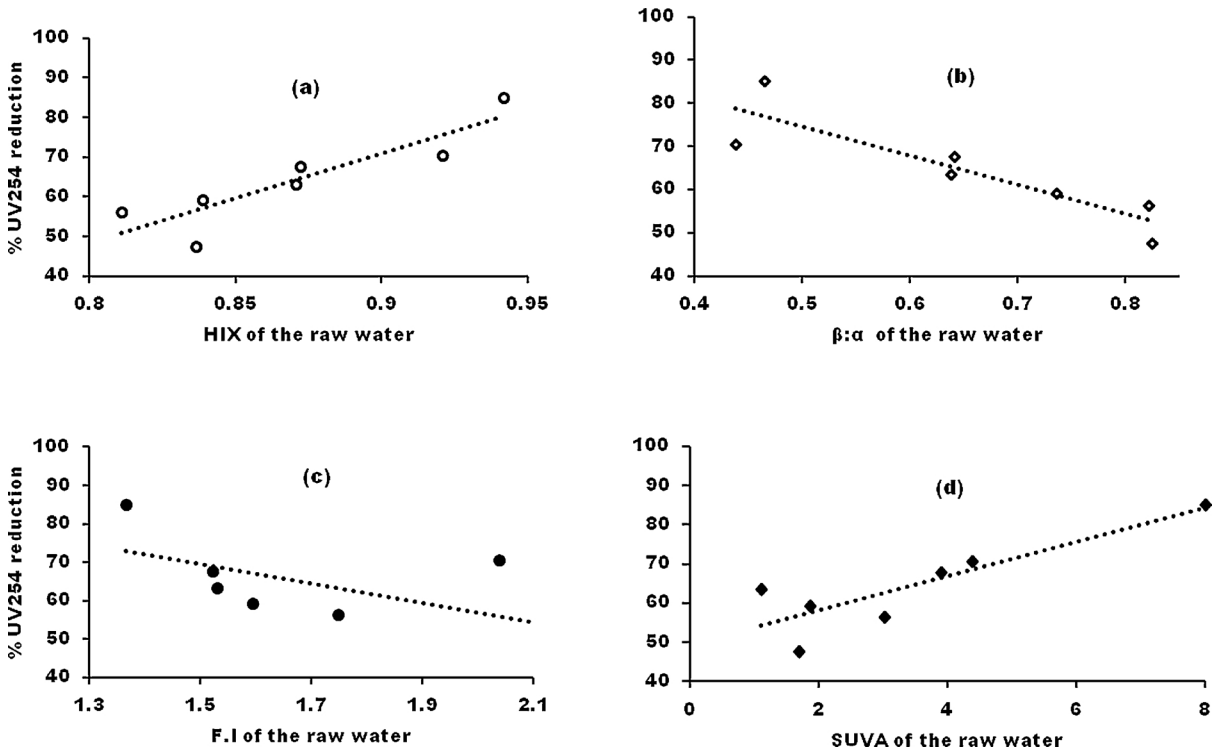

Fig. 5. The variation of UV_{254} reduction as a function of (a) HIX, (b) β:α, (c) FI, and (d) SUVA for the raw water samples.

fulvic material, thus corroborating the SFS results (Section 2.1.2). It is of interest to assess the *Fmax* of the typtophane-like component (C4) because it is a surrogate for wastewater contamination [41]. The trypophane-like component dominated the wastewater effluents unlike the components C1 and C2 which were dorminant in reservoirs and rivers [42]. This is because NOM originating from surface water is predominantly terrestrial mainly from plant matter, whereas sewage-derived NOM mostly originates from autochthonous microbial matter [41]. These distinctions in spectral signatures have facilitated the tracking of wastewater impacted surface waters. Although C4 was always lower than that of any of the other components, its presence signals the impact of wastewater contamination. Plants H and P were less impacted than the other plants because their source waters are less impacted by anthropogenic activities.

3.1.4. Assessment of conventional parameters to evaluate the treatability of NOM at source

Data on physico-chemical properties of NOM is key for the comprehension of its treatability. Source waters had DOC in the range 2.60–12.51 mg/L C (Table 2), which concurs with previous research

that reported that the quantity and quality of NOM have spatial and temporal variability [5]. The measured DOC is what is detected as carbon dioxide after the photo-oxidation of carbon containing organic matter. Therefore, it is not all natural sources of carbon that is measured, instead, runoff of dyes, pesticides and synthetic polymers can exaggerate the obtained values. It is necessary therefore, to further characterize NOM found in surface water. Natural organic matter found in natural waters is the main light absorbing component in the visible range [43]. As expected, the colored raw water laden with humic substances feeding plants H and P showed high UV_{254} absorbance (Table 2). Full UV scans also record absorbance from non-humic substances with high UV–vis absorbance such as inorganic compounds, for example peroxides, nitrates, ammonium [43]. As a result, UV absorbance data in the region < 240 nm is excluded, and instead UV absorbance at 254 nm is used an as indicator for aromaticity [44]. Coastal plants (H and P) showed high UV_{254} absorbance, implying high aromatic content. Other studies have shown that SUVA gives an indication of NOM composition and hence treatment processes can be tailored for its removal [45]. Research has shown that SUVA < 2 L/(mgM) implies the major fraction of NOM in the water is of non-humic substances, and SUVA > 4 L/(mgM) indicates humic substances. Further, DOC > 50% is expected to be removed when SUVA > 4, and < 25% should be removed when SUVA < 2 [46]. Therefore, it is expected that coagulation will remove DOC > 50% in plant H, HL and P; and < 25% from plants FB, UM and MT. Data analysis using Spearman correlation on Xlstat statistical software generated a correlation matrix (Fig A3). As expected, the correlations of spectroscopic parameters were higher with UVA254 than DOC. This is because the non-dispersive infra-red detector (NDIR) that quantifies the DOC measures the concentration of carbon released as carbon dioxide, while UVA254 and spectroscopic ratios measure organic matter moieties that absorb and/or fluoresce in the UV–vis range [40].

3.1.5. Relating optical indices at source to the treatability of natural organic matter

A good correlation between *HIX* and UV_{254} removal was established (R^2 = 0.797) (Fig. 5a). The index *HIX* for raw water gives an indication of NOM removal efficiency [23]. A high *HIX* value means the NOM sample contains high quantities of humic substances. These are easily removed by coagulation in conventional water treatment processes [40]. Thus higher *HIX* should lead to a larger NOM removal. At the same time, the freshness index *(β:α)* was correlated to UV_{254} removal (R^2 = 0.787) (Fig. 5b). A low *β:α* value indicates aged and condensed humic substances susceptible to removal by conventional unit operations such as coagulation [47,20,48]. Microbially derived NOM (*FI* < 1.3) showed greater susceptibility to removal than the terrestrially derived NOM (*FI* > 1.7) (Fig. 5c). Lidén et al., [22] reported similar findings. Interestingly, the correlation of *FI* and *β:α* followed a similar trend. This could be because they are both influenced by microbial derived NOM, either by source (*FI*) or degree of degradation *(β:α)*. Specific UV absorbance showed a mild relationship to the UVA reduction (R^2 = 0.746) (Fig. 5d).

3.2. Selectivite removal of NOM fractions at different stages of the treatment train

3.2.1. Selective removal of biogenic NOM at each treatment stage

The extent of removal of polysaccharides at different stages of the treatment plant as exemplified by plant H is shown in Fig. 6a. The characteristic peak is shown for the differential absorbance scans after each treatment stage. Coagulation removed between -21% (OL) to 15.3% (H) of polysaccaharides. No correlation could be established between polysaccahardes and microbial by-product removal at the coagulation stage. Neither could trends relating spatial locations and polysaccharide treatability be established. This can be attributed to many factors such as coagulant type and charge, pH, and the presence of other charged species that can be entraped within the polysaccharide matrix necessitating its agglomeration into flocs. The negative values for OL (-21%) and FB (−3.7%) indicate a build-up of polysaccharides in the treatment stage. Visual inspection of the abstraction points at these plants showed waxy material characteristic of extracellular polymeric substances (EPS) on the walls of the coagulation/floccultation channels.

High molecular weight (HMW) substances, such as polysaccharides, are generally easily removed in conventional WTPs at the sedimentation stage than low molecular weight (LMW) substances [49]. Therefore the size and type of the polysaccharides detemine its ability to be suspended or to settle at the bottom. While plants in the east coast of South Africa and inland showed similar trend in their ability to remove polysaccharides: HL (22%); AM (22%); MT (19%); UM (18%); OL (21%) and FB (5%), those in the south east coast: H (-5%) and P (-700%) showed a build-up of polysacchaides at the sedimentation stage suggesting their poor settleability.

Polysaccharide reduction at the sand filteration stage correlated well with change in *FI* (R^2 = 0.881) (Fig A. 2b). Because of longer residence times in the sand filter, NOM is usually degraded in sand filters [50]. Unexpectedly, east coast plants perfomed poorly at this stage: HL (−27%); MT (−18%); UM (−12%) and AM (2%), while inland and south east coast plants perfomed better: P (48%); H (25%); FB (17%) and OL (6%). The sand filter is a habitat for many bacterial species which use DOC as a source of nutrients [50]. The assimilability of NOM depends on molecular weight, with heterotrophic bacteria preferentially degrading LMW than HMW NOM [51]. Polysaccarides are macromolecular polymers with high molecular weight (> 20 000 Da), and are not easily assimilable by heterotrophic bacteria [52]. The results suggest that plants in the east coast receive HMW polysaccharides which are not easily degraded by the bacteria.

Polysacaccharide concentration increased at the disinfection stage. This can be attributed to an increase of EPS from bacteria killed during chlorination [13,51]. All plants showed a build-up of polysaccharides at this stage: P (−43%); UM (−36%); AM (−19%); H (−19%); OL (−11%); FB (-7%) and HL (-6%).

3.2.2. Selective removal of chromophoric DOC at each treatment stage

UV-Vis spectra for drinking water samples are nearly featureless except a monotonical absorbance decrease as wavelength increases. Chemometric techniques such as differential spectra (DS) can be used to gain more insights. This tool can present largely comparable features from a UV–vis spectra and can be used to calculate and evaluate the dynamics of CDOM properties after coagulation, sedimentation, rapid sand filtration and disinfection.

The removal by coagulation at shorter wavelengths (< 290 nm) was relatively constant, whereas the removal at longer wavelengths (> 290 nm) shot up by up to 20% (Figure A. 4a). The percent tCDOM removed by coagulation had a correlation coefficient of 0.67 with respect to UV254 removal. This was expected since both these parameters measure the part of NOM that is responsible for fluorescence. Intriguingly, the percent tCDOM removed by coagulation correlated well with percent DOC removed (R^2 = 0.962) (Fig A. 2d). This was unexpected because DOC measures all types of both fluorescent and non fluorescent organic matter [53].

While DOC varied considerably (5–30%) at the sedimentation stage, there was minimum variation of tCDOM (< 10%) (Table A2). This could be because of the phase transformation of particulate organic matter (POM) and NOM as it settles [51]. Sand filtration followed the same trend as sedimentation, with a narrower tCDOM variation (< 5%).

The graph of differential arbsorbance revealed a characteristic absorbance in the region 260–270 nm at the disinfection stage (Fig. 6b). Similar results have been reported in literature [45,18]. Fig. 6c shows a characteristic peak removal from around 260–290 nm of CDOM. These results are consistent with previous findings which reported that the absorbing species in this range are especially reactive during

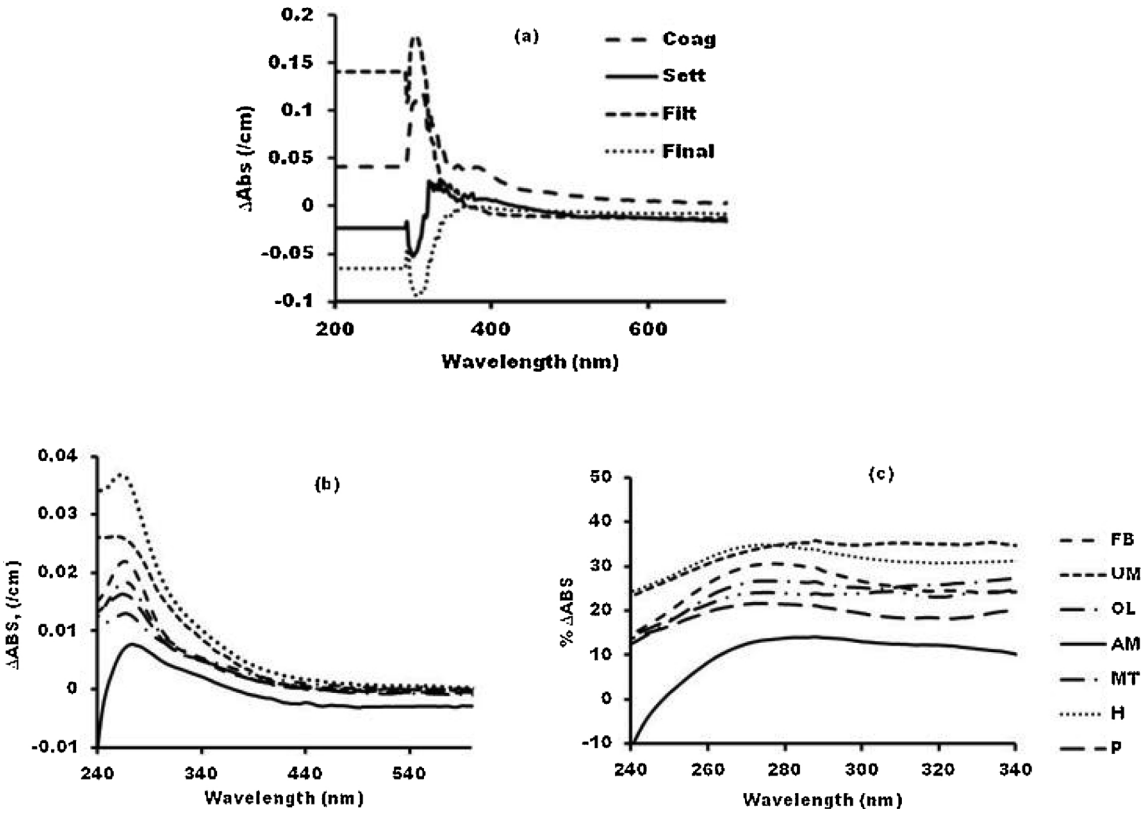

Fig. 6. (a) Differential absorbance as exemplified by H for the removal of polysaccharides throughout the treatment train. (b) Differential absorbance (ΔAbs) during disinfection, (c) % ΔABS removed at the disinfection stage.

chlorination and chloramination [54].

Save for AM, which had accumulation of organic matter, comparison of the DOC removals for the present work and those reported in literature shows the values were generally of the same order of magnitude (Table 3). Membrane filtration and use of nanocomposites were considerably higher, perhaps because these are known to be more effective, and were carried out under optimized laboratory conditions.

3.2.3. Selective removal of fluorescent NOM at each treatment stage

Coagulation was more effective in removing the humic like fractions than the other fractions (Fig. 7a). Bulk DOM removal (in terms of UV254) was higher compared to FDOM in the rapid sand filtration stage, regardless of the location of the plant (Fig. 7b). This suggests that non-FDOM fractions are removed more efficiently than FDOM fractions at the RSF stage. Although the removal of the humic FDOM ($P_{i,5}$) correlated weakly with the SUVA for the raw water ($R^2 = 0.52$), the trend

Table 3
Comparison of DOC removal using different methods.

Removal Method	Removal Efficiency (% DOC)	Remarks	References
• Ion Exchange (IE)	33–41	IE targeted hydrophobic humic (-like) compounds of NOM	[55]
• Electrocoagulation	65	HA-kaolin synthetic solutions	[56]
• AOPs			
UV/H_2O_2	13	Effluent water from a municipal WWTP	[57]
O_3 /H_2O_2	10-15	Natural water from the Otonabee river	Peleato et al., 2017
O_3 /TiO_2	18	Groundwater from the Central Banat province	[58]
Fenton	27.6	Synthetic HA solutions	[59]
Photo-Fenton	15	Surface water from the Pance river	[60]
• Biological degradation	6	Sea water	[61]
• Membrane NF	98-99	Surface water samples	[52]
RO	< 99	Surface water samples	[52]
• Nanocomposites	75	Raw water samples were obtained from the feed water at a WTP	[7]

	Overall		
H	44	Alum (0.061 mg/l)	Current Work*
FB	1	Polymer U38100 (144 mg/L)	
OL	18	Polymer 3546 (4 mg/L)	
MT	64	Zeta-floc (4.6 mg/L0	
AM	−3	Polymer U3500 (8.55 mg/L)	
UM	35	Zeta-floc (4 mg/L)	
HL	24	Polyamine (3.3 mg/L)	
P	42	SUD-floc (0.006 mg/L)	

* Calculated from removals at coagulation, clarification, sand filtration, and disinfection unit operations.

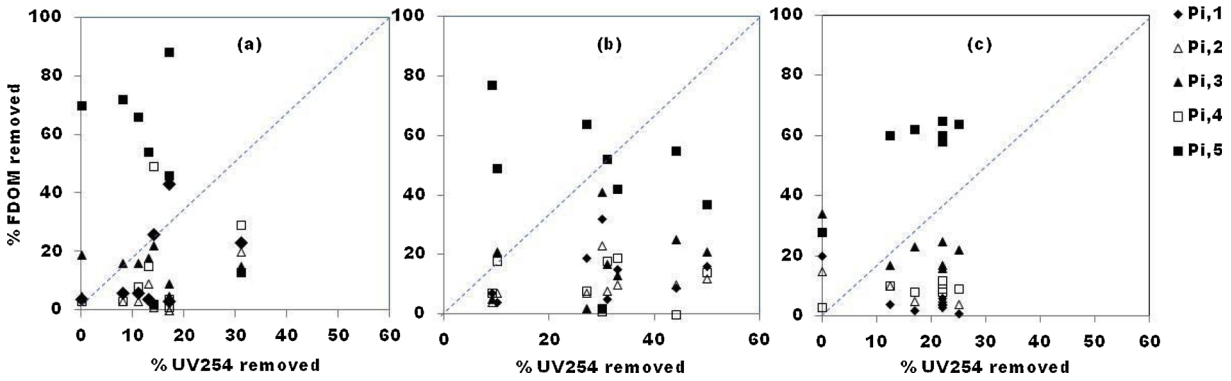

Fig. 7. Correlations between the removal FDOM and the removal of NOM in three treatment stages (a) coagulation, (b) slow sand filtration, and (c) disinfection.

was nonetheless, in agreement with the findings that SUVA > 4 results in more than 50% removal of humics by coagulation. For example, plant H had a SUVA of 15.63 at source and a humics removal of 88% by coagulation. Although disinfection was efficient in removing humic-like fractions, its efficiency on removing other FDOM fractions was low (Fig. 7c). Chlorination results in the chemical modification of NOM by selectively targeting double bonds and conjugated functional groups. Depending on the number and distribution of these moieties, there are differential removal rates of bulk NOM and FNOM, and differential generation of DBPs (Chen et al., 2003). Overall, despite the total removal efficiencies of humic-like FNOM being high, removal efficiencies for other FNOM fractions were much lower. This indicates the drinking water treatment processes are less effective in removing FNOM compared to bulk NOM.

FNOM can be rapidly and sensitively detected online by fluorescence spectroscopy techniques [32,48]. An understanding of the dynamics of FNOM fractions in drinking water production is necessary for monitoring and control since the overall removal of NOM is strongly correlated to its fluorescent fractions [28,51].

4. Conclusion

The study investigated the concentration and chemical profile of NOM in drinking water treatment sources in South Africa, as well as the fate of NOM and its transformations throughout the treatment train at various plants. This is the first such study conducted in South Africa to determine the occurrence, behaviors and removal efficiencies of fluorescent EEM components by the country's water treatment plants. Water samples were analyzed for DOC, UV absorbance, SUVA, spectroscopic indices, fluorescence intensity as well as biopolymer (polysaccharides), and the following key findings were reported:

1 The character of NOM with respect to SUVA served as a prediction for its removal. As expected, coagulation removed DOC > 50% in plants: H, HL and P which had SUVA > 4; and < 25% DOC removal was observed from plants FB, UM and MT, which had a SUVA < 2.
2 A model fitting four components was crafted and validated based on the split half criteria, the distribution of the components at each water source was quantified using their maximum fluorescence intensities *(Fmax)*. The value of *Fmax* was higher for the terrestrial humic-like component (C1) and the fulvic like component (C2) than for humic-like components (C3), and for protein-like (C4) components, suggesting C1 and C2 have higher quantum efficiencies and lower responses to quenching effects compared to C3 and C4.
3 Coagulation was more effective in removing the humic like fractions than the other fractions. Bulk DOM removal (with respect to UV254) was higher compared to FDOM in the rapid sand filtration stage, regardless of location of the plant. This suggests that non-FDOM fractions are removed more efficiently than FDOM fraction at the RSF stage. Although disinfection was efficient in removing humic like fractions, its efficiency on removing other FDOM was low.

Acknowledgements

The authors are grateful for funding received from the National Research Foundation (NRF), South Africa, the Water Research Commission (WRC) of South Africa, and the University of South Africa.

Appendix A. Supplementary data

Supplementary material related to this article can be found, in the online version, at doi:https://doi.org/10.1016/j.jece.2019.103101.

References

[1] N.P. Sanchez, A.T. Skeriotis, C.M. Miller, Assessment of dissolved organic matter fluorescence PARAFAC components before and after coagulation e filtration in a full scale water treatment plant, Water Res. 47 (4) (2013) 1679–1690, https://doi.org/10.1016/j.watres.2012.12.032.
[2] J.P. Crou, G.V. Korshin, M.M. Benjamin, Characterization of Natural Organic Matter in Drinking Water, American Water Works Association Reseach Foundation (AWWARF), 2000.
[3] X. Booi, Perfluorinated Compounds and Trihalomethanes in Drinking Water Sources of the Western Cape, South Africa. Masters Dissertation, Cape Peninsula University of Technology, 2013.
[4] E. Brooks, C. Freeman, R. Gough, P.J. Holliman, Tracing dissolved organic carbon and trihalomethane formation potential between source water and fi nished drinking water at a lowland and an upland UK catchment, Sci. Total Environ. 537 (2015) 203–212, https://doi.org/10.1016/j.scitotenv.2015.08.017.
[5] T.I. Nkambule, R.W.M. Krause, J. Haarhoff, B.B. Mamba, A three step approach for removing organic matter from South African water sources and treatment plants, Phys. Chem. Earth 50–52 (2012) 132–139, https://doi.org/10.1016/j.pce.2012.08.009.
[6] S.S. Marais, E.J. Ncube, T.A.M. Msagati, J. Haarholff, T.I. Nkambule, Characterization and removal of natural organic matter by a water treatment plant in South Africa, Specialist Conference on Natural Organic Matter in Drinking Water (2015).
[7] N. Chaukura, W. Moyo, T.A.M. Msagati, B.B. Mamba, Thabo I. Nkambule, Removal of dissolved organic matter from raw water using zero valent iron -carbonaceous conjugated microporous polymer nanocomposites, Phys. Chem. Earth 107 (2018) 38–44, https://doi.org/10.1016/j.pce.2018.08.006.
[8] J. Haarhoff, B.B. Mamba, R. Krause, Staden S. van, T.I. Nkambule, S. Dlamini, K.P. Lobanga, Natural Organic Matter in Drinking Water Sources: Its Characterisation and Treatability. *WRC report*. Report number. 1883/1/12, (2013).
[9] K.R. Murphy, C. Stedmon, D. Graeber, R. Bro, Fluorescence spectroscopy and multi-way techniques. PARAFAC, Anal. Methods 5 (23) (2013) 6557, https://doi.org/10.1039/c3ay41160e.
[10] K. Ozdemir, Characterization of natural organic matter in conventional water treatment processes and evaluation of THM formation with chlorine, Sci. World J. 2014 (2014), https://doi.org/10.1155/2014/703173.
[11] M. Sgroi, P. Roccaro, G.V. Korshin, V. Greco, S. Sciuto, T. Anumol, S. Snyder, F.G.A. Vagliasindi, Use of fluorescence EEM to monitor the removal of emerging contaminants in full scale wastewater treatment plants, J. Hazard. Mater. 323 (2017) 367–376, https://doi.org/10.1016/j.jhazmat.2016.05.035.
[12] R.H. Peiris, M. Jaklewicz, H. Budman, R.L. Legge, C. Moresoli, Characterization of hydraulically reversible and irreversible fouling species in ultra fi ltration drinking water treatment systems using fluorescence EEM and LC – OCD measurements, J. Water Supply Res. Technol. 13 (5) (2013) 1220–1227, https://doi.org/10.2166/ws.2013.130.

[13] J. Sun, L. Guo, Q. Li, Y. Zhao, M. Gao, Z. She, C. Jin, Three-dimensional fluorescence excitation–emission matrix (EEM) spectroscopy with regional integration analysis for assessing waste sludge hydrolysis at different pretreated temperatures, Environ. Sci. Pollut. Res. - Int. 23 (23) (2016) 24061–24067, https://doi.org/10.1007/s11356-016-7610-4.

[14] M. Park, S.A. Snyder, Chemosphere Sample handling and data processing for fl uorescent excitation- emission matrix (EEM) of dissolved organic matter (DOM), Chemosphere 193 (2018) 530–537, https://doi.org/10.1016/j.chemosphere.2017.11.069.

[15] Q. Viet, H. Kim, J. Hur, Tracking fl uorescent dissolved organic matter in hybrid ultra fi ltration systems with TiO 2 / UV oxidation via EEM-PARAFAC, J. Membr. Sci. 549 (2018) 275–282, https://doi.org/10.1016/j.memsci.2017.12.020.

[16] U.J. Wu, K.R. Murphy, C.A. Stedmon, The one-sample PARAFAC approach reveals molecular size distributions of fluorescent components in dissolved organic matter, Environ. Sci. Technol. 51 (20) (2017) 11900–11908, https://doi.org/10.1021/acs.est.7b03260.

[17] J.R. Helms, A. Stubbins, J.D. Ritchie, e.C. Minor, D.J. Kieber, K. Mopper, Absorption spectral slopes and slope ratios as indicators of molecular weight, source, and photobleaching of chromophoric dissolved organic matter, Limnol. Oceanogr. 53 (3) (2008) 955–969, https://doi.org/10.4319/lo.2008.53.3.0955.

[18] W.T. Li, M.J. Cao, T. Young, B. Ruffino, M. Dodd, A.M. Li, G. Korshin, Application of UV absorbance and fluorescence indicators to assess the formation of biodegradable dissolved organic carbon and bromate during ozonation, Water Res. 111 (2017) 154–162, https://doi.org/10.1016/j.watres.2017.01.009.

[19] T.I. Nkambule, Natural Organic Matter (Nom) in South African Waters: Characterization of Nom, Treatability and Method Development for Effective Nom Removal From Water. PhD Thesis, University of Johannesburg, 2012.

[20] K.P. Lobanga, Natural Organic Matter Removal From Surface Waters by Enhanced Coagulation, Granular Activated Carbon Adsorption and Ion Exchange. PhD Thesis, University of Johannesburg, 2012.

[21] N. Chaukura, N.G. Ndhlangamadhla, W. Moyo, T.A.M. Msagati, B.B. Mamba, T.I. Nkambule, Natural organic matter in aquatic systems - a South African perspective, Water SA 44 (4) (2018) 624–635.

[22] A. Lidén, A. Keucken, K.M. Persson, Uses of fluorescence excitation-emissions indices in predicting water treatment efficiency, J. Water Process. Eng. 16 (2017) 249–257, https://doi.org/10.1016/j.jwpe.2017.02.003.

[23] X.S. He, B.D. Xi, X. Li, H.W. Pan, D. An, S.G. Bai, D. Li, d an, D.Y. Cui, Fluorescence excitation-emission matrix spectra coupled with parallel factor and regional integration analysis to characterize organic matter humification, Chemosphere 93 (9) (2013) 2208–2215, https://doi.org/10.1016/j.chemosphere.2013.04.039.

[24] A.A. Albalasmeh, A.A. Berhe, T.A. Ghezzehei, A new method for rapid determination of carbohydrate and total carbon concentrations using UV spectrophotometry, Carbohydr. Polym. 97 (2) (2013) 253–261, https://doi.org/10.1016/j.carbpol.2013.04.072.

[25] G.V. Korshin, C.W. Li, M.M. Benjamin, Monitoring the properties of natural organic matter through UV spectroscopy : a consistent theory, Water Res. 31 (7) (1997) 1787–1795, https://doi.org/10.1016/S0043-1354(97)00006-7.

[26] P. Li, J. Hur, Utilization of UV-Vis spectroscopy and related data analyses for dissolved organic matter (DOM) studies: a review, Crit. Rev. Environ. Sci. Technol. 47 (3) (2017) 131–154, https://doi.org/10.1080/10643389.2017.1309186.

[27] G.V. Korshin, J.P. Croue, C.W. Li, M.M. Benjamin, Comprehensive study of uv absorption and fluorescence spectra of Suwannee river nom fractions, Seattle, W. And Seattle, W, Understanding Humic Substances, (1999), https://doi.org/10.1016/B978-1-85573-815-7.50019-2.

[28] H. Yu, F. Qu, H. Chang, S. Shao, X. Zou, G. Li, H. Liang, Understanding ultrafiltration membrane fouling by soluble microbial product and effluent organic matter using fluorescence excitation-emission matrix coupled with parallel factor analysis, Int. Biodeterior. Biodegrad. 102 (2015) 56–63, https://doi.org/10.1016/j.ibiod.2015.01.011.

[29] S. Meng, W. Fan, X. Li, Y. Liu, D. Liang, X. Liu, Intermolecular interactions of polysaccharides in membrane fouling during micro filtration, Water Res. 143 (2018) 38–46, https://doi.org/10.1016/j.watres.2018.06.027.

[30] J. Hur, K. Jung, Y. Mee, Characterization of spectral responses of humic substances upon UV irradiation using two-dimensional correlation spectroscopy, Water Res. 45 (9) (2011) 2965–2974, https://doi.org/10.1016/j.watres.2011.03.013.

[31] H. Yu, Y. Song, X. Tu, E. Du, R. Liu, J. Peng, Assessing removal efficiency of dissolved organic matter in wastewater treatment using fluorescence excitation emission matrices with parallel factor analysis and second derivative synchronous fluorescence, Bioresour. Technol. 144 (2013) 595–601, https://doi.org/10.1016/j.biortech.2013.07.025.

[32] H. Yu, B. Xi, W. Ma, D. Li, X. He, Fluorescence spectroscopic properties of dissolved fulvic acids from salined flavo-aquic soils around Wuliangsuhai in Hetao Irrigation District, China, Soil Sci. Soc. Am. 75 (4) (2011) 1385–1393, https://doi.org/10.2136/sssaj2010.0373.

[33] K. Kaibitz, W. Geyer, S. Geyer, Spectroscopic properties of dissolved humic substatncies - a reflection of land use history in a fen area, Biogeochemistry 47 (2) (1999) 219–238, https://doi.org/10.1007/BF00994924.

[34] K. Kimura, Y. Oki, Efficient control of membrane fouling in MF by removal of biopolymers: comparison of various pretreatments, Water Res. 115 (2017) 172–179, https://doi.org/10.1016/j.watres.2017.02.033.

[35] K. Kimura, K. Shikato, Y. Oki, K. Kume, S.A. Huber, Surface water biopolymer fractionation for fouling mitigation in low-pressure membranes, J. Memb. Sci. 554 (2018) 83–89, https://doi.org/10.1016/j.memsci.2018.02.024.

[36] Z. Filip, W. Pecher, J. Berthelin, Microbial utilization and transformation of humic acid-like substances extracted from a mixture of municipal refuse and sewage sludge disposed of in a landfill, Environ. Pollut. 109 (1) (2000) 83–89, https://doi.org/10.1016/S0269-7491(99)00229-8.

[37] X. Li, M. Xing, J. Yang, Z. Huang, Compositional and functional features of humic acid-like fractions from vermicomposting of sewage sludge and cow dung, J. Hazard. Mater. 185 (2–3) (2011) 740–748, https://doi.org/10.1016/j.jhazmat.2010.09.081.

[38] K.R. Murphy, C.A. Stedmon, P. Wening, R. Bro, Analytical Methods OpenFluor – an online spectral library of auto- fl uorescence by organic compounds in the environment, Anal. Methods 6 (2014) 658–661, https://doi.org/10.1039/c3ay41935e.

[39] S.N. Ndiweni, M. Chys, N. Chaukura, S.W.H. Van Hulle, T.I. Nkambule, Assessing the impact of environmental activities on natural organic matter in South Africa and Belgium, Environ. Technol. (2019), https://doi.org/10.1080/09593330.2019.1575920.

[40] S.A. Baghoth, S.K. Sharma, G.L. Amy, Tracking natural organic matter (NOM) in a drinking water treatment plant using fluorescence excitation emission matrices and PARAFAC, Water Res. 45 (2) (2010) 797–809, https://doi.org/10.1016/j.watres.2010.09.005.

[41] R.K. Henderson, A. Baker, K.R. Murphy, A. Hamply, R.M. Stuetz, S.J. Khan, Fluorescence as a potential monitoring tool for recycled water systems : a review, Water Res. 43 (4) (2009) 863–881, https://doi.org/10.1016/j.watres.2008.11.027.

[42] A.D. Pifer, J.L. Fairey, Suitability of organic matter surrogates to predict trihalomethane formation in drinking water sources, Environ. Eng. Sci. 31 (3) (2014) 117–126, https://doi.org/10.1089/ees.2013.0247.

[43] D.J. Dryer, G.V. Korshin, M. Fabbricino, In situ examination of the protonation behavior of fulvic acids using differential absorbance spectroscopy, Environ. Sci. Technol. 42 (17) (2008) 6644–6649, https://doi.org/10.1021/es800741u.

[44] G.S. Wang, S.T. Hsieh, Monitoring natural organic matter in water with scanning spectrophotometer, Environ. Int. 26 (4) (2001) 205–212, https://doi.org/10.1016/S0160-4120(00)00107-0.

[45] P. Roccaro, M. Yan, G.V. Korshin, Use of log-transformed absorbance spectra for online monitoring of the reactivity of natural organic matter, Water Res. 84 (2015) 136–143, https://doi.org/10.1016/j.watres.2015.07.029.

[46] E. Lavonen, Tracking Changes in Dissolved Natural Organic Matter Composition. Doctoral Thesis, Swedish University of Agricultural Sciences, 2015.

[47] T. Meyn, J. Altmann, T.O. Leiknes, Direct Surface Water Treatment With coagulation/ceramic Microfiltration - Minimisation of Flocculation Pre-treatment, Desalination and Water Treatment, (2011) Available at: (Accessed 03/11/2018) http://www.diva-portal.org/smash/record.jsf?pid=diva2:451826&dswid=-9316.

[48] D. Zheng, R.C. Andrews, S.A. Andrews, Taylor-Edmonds, Effects of coagulation on the removal of natural organic matter, genotoxicity, and precursors to halogenated furanones, Water Res. 70 (2015) 118–129, https://doi.org/10.1016/j.watres.2014.11.039.

[49] Z. Su, T. Liu, W. Yu, X. Li, N.J. Graham, Coagulation of surface water : observations on the significance of biopolymers, Water Res. 126 (2017) 144–152, https://doi.org/10.1016/j.watres.2017.09.022.

[50] E. Prest, F. Hammes, M.C.M. van Loosdrecht, J.S. Vrouwenvelder, Biological stability of drinking water : controlling factors, methods, and challenges, Front. Microbiol. 7 (45) (2016) 1–24, https://doi.org/10.3389/fmicb.2016.00045.

[51] X. Yang, Z. Zhou, M.N. Raju, X. Cai, and Meng F, Selective elimination of chromophoric and fluorescent dissolved organic matter in a full-scale municipal wastewater treatment plant, J. Environ. Sci. (China) 57 (2017) 150–161, https://doi.org/10.1016/j.jes.2016.11.003.

[52] J. Shen, A.I. Schafer, Factors affecting fluoride and natural organic matter (NOM) removal from natural waters in Tanzania by nanofiltration/reverse osmosis, Sci. Total Environ. 2015 (2015) 520–529, https://doi.org/10.1016/j.scitotenv.2015.04.037.

[53] S.A. Baghoth, Characterizing Natural Organic Matter in Drinking Water Treatment Processes and Trains. PhD Thesis, Technical University of Delft, 2012.

[54] E.E. Lavonen, D.N. Kothawala, L.J. Tranvik, M. Gosior, P. Schmitt-Kopplin, S.J. Kohler, Tracking changes in the optical properties and molecular composition of dissolved organic matter during drinking water production, Water Res. 85 (2015) 286–294, https://doi.org/10.1016/j.watres.2015.08.024.

[55] M.M. Bazri, B. Martijn, J. Kroesbergen, M. Mohseni, Impact of anionic ion exchange resins on NOM fractions: effect on N-DBPs and C-DBPs precursors, Chemosphere 144 (2016) 1988–1995.

[56] C. Hu, S. Wang, J. Sun, H. Liu, J. Qu, An effective method for improving electrocoagulation process: optimization of Al_{13} polymer formation, Colloids Surf. A Physicochem. Eng. Asp. 489 (2016) 234–240, https://doi.org/10.1016/j.colsurfa.2015.10.063.

[57] W.T.M. Audenaert, D. Vandierendonck, S.W.H. Van Hulle, I. Nopens, Comparison of ozone and HO induced conversion of effluent organic matter (EfOM) using ozonation and UV/H2O2 treatment, Water Res. 47 (7) (2013) 2387–2398.

[58] J. Molnar, J. Agbaba, B. Dalmacija, M. Klasnja, M. Dalmacija, M. Kragulj, A comparative study of the effects of ozonation and TiO2-catalyzed ozonation on the selected chlorine disinfection by-product precursor content and structure, Sci. Total Environ. 425 (2012) 169–175.

[59] H.B. Wu, H.H. Hng, X.W.D. Lou, Direct synthesis of anatase TiO2 nanowires with enhanced photocatalytic activity, Adv. Mater. 24 (19) (2012) 2567–2571.

[60] A. Moncayo-Lasso, A.G. Rincon, C. Pulgarin, N. Benitez, Significant decrease of THMs generated during chlorination of river water by previous photo-Fenton treatment at near neutral pH, J. Photochem. Photobiol. A: Chem. 229 (1) (2012) 46–52.

[61] F.X. Simon, E. Rude, J. Liorens, S. Baig, Study on the removal of biodegradable NOM from seawater using biofiltration, Desalination 316 (2013) 8–16.